Targ Oncol (2015) 10:215–227
DOI 10.1007/s11523-014-0323-z

ORIGINAL RESEARCH

Side population cells of pancreatic cancer show characteristics of cancer stem cells responsible for resistance and metastasis

Hanno Niess · Peter Camaj · Andrea Renner · Ivan Ischenko · Yue Zhao · Stefan Krebs · Josef Mysliwietz · Carsten Jäckel · Peter J. Nelson · Helmut Blum · Karl-Walter Jauch · Joachim W. Ellwart · Christiane J. Bruns

Received: 19 November 2013 / Accepted: 9 May 2014 / Published online: 22 June 2014

Abstract Cancer stem cells (CSCs) have been proposed to underlie the initiation and maintenance of tumor growth and the development of chemoresistance in solid tumors. The identification and role of these important cells in pancreatic cancer remains controversial. Here, we isolate side population (SP) cells from the highly aggressive and metastatic human pancreatic cancer cell line L3.6pl and evaluate their potential role as models for CSCs. SP cells were isolated following Hoechst 33342 staining of L3.6pl cells. SP, non-SP, and unsorted L3.6pl cells were orthotopically xenografted into the pancreas of nude mice and tumor growth observed. RNA was analyzed by whole genome array and pathway mapping was performed. Drug resistant variants of L3.6pl were developed and examined for SP proportions and evaluated for surface expression of known CSC markers. A distinct SP with the ability to self-renew and differentiate into non-SP cells was isolated from L3.6pl (0.9 %±0.22). SP cells showed highly tumorigenic and metastatic characteristics after orthotopic injection. Transcriptomic analysis identified modulation of gene networks linked to tumorigenesis, differentiation, and metastasization in SP cells relative to non-SP cells. Wnt, NOTCH, and EGFR signaling pathways associated with tumor stem cells were altered in SP cells. When cultured with increasing concentrations of gemcitabine, the proportion of SP cells, $ABCG2^+$, and $CD24^+$ cells were significantly enriched, whereas 5-fluorouracil (5-FU) treatment lowered the percentage of SP cells. SP cells were distinct from cells positive for previously postulated pancreatic CSC markers. The Hoechst-induced side population in L3.6pl cells comprises a subset of tumor cells displaying aggressive growth and metastasization, increased gemcitabine-, but not 5-FU resistance. The cells may act as a partial model for CSC biology.

Keywords Pancreatic cancer · Cancer stem cells · Tumor-initiating cells · Side-population · Chemotherapy resistance · ABCG2 · Pathway mapping · Aldoketoreductase family 1 B10

This research was supported by the FöFoLe Research Program (no. 570/548/636) of the University of Munich, Munich, Germany and the SPP1190/2 "Tumor vessel interface" (BR 1614/8-2) of the German Research Society (DFG).

All animal experiments were performed in accordance with institutional and governmental guidelines and approval obtained from the ethics commission of the State of Bavaria (no. 55.2-1-54-2531-19-08).

Electronic supplementary material The online version of this article (doi:10.1007/s11523-014-0323-z) contains supplementary material, which is available to authorized users.

H. Niess · A. Renner · I. Ischenko · K.-W. Jauch
Department of Surgery, University of Munich, Campus Großhadern, Munich, Germany

S. Krebs · H. Blum
Laboratory for Functional Genome Analysis, University of Munich, Munich, Germany

J. Mysliwietz · J. W. Ellwart
Institute of Molecular Immunology, Helmholtz Center for Environment and Health, Munich, Germany

C. Jäckel · P. J. Nelson
Medizinische Klinik und Poliklinik IV, University of Munich, Campus Innenstadt, Munich, Germany

P. Camaj · Y. Zhao · C. J. Bruns (✉)
Department of Surgery, Otto-von-Guericke-University, Leipziger Str. 44, Haus 60a, 39120 Magdeburg, Germany
e-mail: Christiane.bruns@med.ovgu.de

Introduction

Advances in the field of cancer and stem cell biology have led to formulation of the cancer stem cell hypothesis [1]. This hypothesis stands in contrast to the clonal hypothesis of tumor development [2] and proposes that heterogeneous, clonal

cancer cells arise from a single or subset of transformed tissue stem cells, called cancer stem cells (CSC). CSCs are, like adult stem cells, thought to be capable of self-renewal and differentiation into adult progeny (asymmetric cell division). Thus, it has been proposed that CSCs maintain the pool of cancer stem cells just as they represent the source of the diverse tumor cells contained in a solid tumor bulk [3].

CSCs are hypothesized to be responsible for several malignant aspects of tumor growth such as resistance to chemotherapy and radiation, invasion, and metastasis. By expression of multiple drug resistance transporters (MDR), CSCs are capable of effluxing several chemotherapeutic agents from the cell and thus are responsible for tumor recurrence [4]. Their resistance to radiation therapy is thought to lie in the enhanced capacity of their DNA repair mechanisms [5]. The migratory capacity of tissue stem cells and expression of receptors involved in cell trafficking, support the hypothesis of CSCs as the origin of distant metastases of tumors [6]. Taken together, the CSC hypothesis implies that treatments specifically targeting the CSC population of tumors will be required in order to achieve an effective and stable cure for cancer.

Putative CSCs have been documented in hematopoietic malignancies, brain cancer, and solid organ malignancies including breast, prostate, and colon cancer [6–8]. Recently, the stem cell hypothesis has been explored for human pancreatic cancer [9–11]. In the search for putative CSCs, different strategies to describe and distinguish these cells have been applied. The expression of specific surface markers describing the phenotype of these cells has been used for characterization. In this manner, pancreatic CSCs were described as expressing CD44, CD24, and epithelial specific antigen (ESA) [12]. A second study identified pancreatic cancer cell populations with stem cell characteristics that showed increased expression of CD133 and CXCR4 [13]. However, the biological function of the respective surface markers and their contribution to "stemness" of the expressing cell remains unclear in most cases.

Putative CSCs have been isolated from the bulk of tumor cells based on their ability efflux chemotherapeutics and by extrapolation Hoechst 33342 dye [14]. In the present study, side population cells were isolated from a highly aggressive human pancreatic cancer cell line and characterized for their tumorigenicity and general characteristics linked to CSC-associated biology. The SP cells demonstrate features associated with CSC biology and as such may represent a tool for the further characterization of this important cell type.

Materials and methods

Human pancreatic cancer cells and culture conditions

The human pancreatic adenocarcinoma cell line L3.6pl [15] was used to develop gemcitabine- and 5-fluorouracil (5-FU)-resistant cell lines (L3.6pl-Gem_{res} and L3.6pl-5-FU_{res}). To this end, L3.6pl were cultured in medium with increasing concentrations of gemcitabine (Gemzar; Lilly Deutschland GmbH, Gießen, Germany), starting at 0.5 ng/ml up to 7.5 ng/ml or 5-FU (Fluorouracil-GRY, TEVA Deutschland GmbH, Mörfelden-Walldorf), starting at 0.18 μg/ml up to 0.54 μg/ml. Media was exchanged three times a week. Cell lines were maintained in Dulbecco's Minimal Essential Medium (D-MEM; Invitrogen GmbH, Karlsruhe, Germany), supplemented with 10 % fetal bovine serum (Biochrom AG, Berlin, Germany), 2 % MEM vitamin mixture (PAN Biotech GmbH, Aidenbach, Germany), 2 % MEM NEAA (PAN Biotech GmbH, Aidenbach, Germany), 1 % penicillin streptomycin (PAN Biotech GmbH, Aidenbach Germany), and 2 % glutamax (Invitrogen GmbH, Karlsruhe, Germany). Cells were incubated in a humidified incubator (37ºC, 5 % CO_2), grown in cell culture flasks, and passaged on reaching 70–80 % confluence.

Analysis of SP and non-SP cell fractions from L3.6pl, L3.6pl-Gem_{res} and L3.6pl-5-FU_{res} cell lines

SP and non-SP cell fractions were identified and isolated using a modified protocol described by Goodell et al. [14]. Briefly, cells were resuspended at 37ºC in D-MEM containing 2 % fetal bovine serum and labeled with Hoechst 33342 (Sigma-Aldrich GmbH, Steinheim, Germany) at a concentration of 2.6 μg/ml for 60 min at 37ºC, either alone or with 225 μM verapamil hydrochloride (Sigma-Aldrich GmbH, Steinheim, Germany). After staining, the cells were centrifuged at 4 °C and 300×*g* for 5 min and resuspended in ice cold PBS, containing 2 % fetal bovine serum, passed through a 35 μm mesh filter and maintained at 4ºC in the dark until flow cytometry analysis or further cell surface marker staining. Cells were counterstained with 10 μg/ml propidium iodide to label dead cells, then analyzed by BD-LSRII flow cytometer (BD Biosciences, Heidelberg, Germany) and FlowJo software (Treestar Inc., Ashland, USA), or sorted by MoFlo with the Summit 4.3 software (Beckmann coulter GmbH, Krefeld, Germany). Hoechst dye was excited at 355 nm (UV), and the fluorescence was measured at two wavelengths using a 450/50 nm (blue) band-pass filter and a 670/30 nm (red) long-pass edge filter. After isolation, SP and non-SP cell fractions were cultivated for two weeks at the same conditions and passaged two times before reanalysis.

Cell proliferation assay and IC_{50} determination

Cell proliferation was measured using the TACS MTT cell proliferation and viability assay kit (R&D systems, Minneapolis, USA) used according to the manufacturer's instructions. Briefly, 8,000 cells/well plated on a 96-well plate were grown overnight, treated for 24 h with chemotherapeutics, and

analyzed afterwards using VersaMax tunable microplate reader and Softmaxpro 5.2 (Molecular devices, Sunnyvale, USA).

Analysis of the tumor-initiating capability of SP and non-SP cells in vivo

For analysis of orthotopic tumor growth, isolated SP and non-SP cells as well as unsorted L3.6pl cells were injected into the pancreas of male athymic BALB/c nu/nu mice (Charles River WIGA, Sulzfeld, Germany), as described previously [15]. Tumor cell injection and tumor evaluation was carried out in a blinded manner. A left abdominal flank incision was made, the spleen was exteriorized, and 10^5 cells were injected into the subcapsular region of the pancreas. Orthotopic tumor growth was monitored longitudinally by estimation of tumor volume using transcutaneous palpation and caliper measurement every 3–4 days. On day 34 after tumor cell implantation, animals were sacrificed and examined for orthotopic tumors, lymph node, and hepatic metastases. The tumor volume was calculated using the formula $V=a\times b\times c\times 0.52$ with a, b, and c representing length, width, and height of the tumor, respectively.

Conservation of tissue samples in paraffin wax and H&E staining

Following sacrifice, tissue samples were maintained in 4 % neutral buffered formaldehyde for 24 h before rinsing with water for 1 h. Samples were then dehydrated in ascending ethanol series (70 %, 96 %, 100 %), xylol, and finally coated in paraffin wax. For H&E staining, samples were deparaffinized by incubation at 60 °C for 10 min, followed by incubation for 20 min in xylol, 10 min in 100 % EtOH, 3 min in 96 % EtOH, 3 min in 70 % EtOH, and finally washed in distilled water. Samples were then plunged in hematoxylin for 1–3 min, washed in distilled water, and incubated with eosin for 8–12 min. After dehydrogenation for a few seconds in 80 % EtOH, 30 s in 90 % EtOH, 30 s in 96 % EtOH, 4 min in 100 % EtOH, and 10 min in xylol, the slides were mounted in eukitt.

RNA sample preparation for microarray hybridization

Immediately after fluorescence-assisted sorting into ice-chilled PBS containing 2 % FCS, the cells were centrifuged, resuspended in TriFast (PEQLAB Biotechnologie GMBH, Erlangen, Germany), and frozen at −80 °C until RNA isolation. Total RNA was isolated from the TriFast suspension following the standard method. However, as the small amounts of RNA retrieved from side-population cells showed significant contaminations of residual TriFast reagent, it was subjected to extraction with N-Butanol as already described [16]. After the extraction, all total RNA samples showed sufficient purity and RNA integrity for microarray hybridization as assessed by spectrophotometry (Nanodrop, Wilmington, DE, USA) and electrophoresis (agarose gel electrophoresis and Agilent Bioanalyzer).

Microarray hybridization

One hundred nanograms of total RNA were used to prepare labeled cDNA fragments for hybridization on Affymetrix HuGene 1.0 ST microarrays. Briefly, total RNA was reversely transcribed to cDNA, in vitro transcribed to cRNA that was reversely transcribed again, fragmented, and terminally labeled. All steps were performed using the GeneChip® WT Sense Target Labeling Kit (Affymetrix, Santa Clara, California, USA) following the manufacturer-provided protocol. Labeled probes were hybridized to HuGene ST 1.0 arrays at a final concentration of 25 ng/µl for 16 h at 45 °C. The arrays were washed and stained on a FluidicStation F450 (Affymetrix, Santa Clara, CA, USA).

Microarray analysis

The fully processed microarrays were scanned (Affymetrix Gene Chip Scanner 3000) and the CEL-files were read into the Bioconductor R workspace using the R package xps for background correction, normalization, and quality control [17]. The xps package provides an adaption of the RMA normalization to Gene ST 1.0 arrays which was used here [18]. After normalization, differentially expressed genes were identified using the R-package LIMMA [19]. Briefly, a moderated *t* test with Benjamini-Hochberg correction was used and only corrected *p* values below 0.01 were considered. Differential expression was further restricted to a $\log_2$ fold change larger than 1.

Additional quality control and clustering analyses were carried out using the Management and Analysis Database for Multi-platform microArray eXperiments (MADMAX) platform (https://madmax.bioinformatics.nl, University of Wageningen), while normalizing the data using the gcRMA algorithm.

The data was then analyzed using Genomatix ChipInspector and Genomatix Pathway System (GePS) (Genomatix Software GmbH, Munich). ChipInspector utilizes a single probe approach for significance analysis and normalization, in contrast to RMA which works with chip-wide averages. The parameters used were the following: positive delta 0.74, negative delta −0.61, False Discovery Rate (FDR) of 0 %, region size 300 bp, and with no fold change-based cutoff criteria. After significance analysis, the filtered gene lists are grouped into biological pathways using GePS, and these pathways were then scored by the level of dysregulated genes. This approach allows for discovery of the most dramatically changed processes even within large datasets [20, 21].

Comparisons of Genomatix and gcRMA data for individual genes were performed to increase confidence in the results.

Analysis of protein expression by Western blot

Cells were sorted into ice cold PBS containing 2 % fetal bovine serum and resuspended in ice cold RIPA buffer supplemented with the cocktail of protease/phosphotase inhibitors (Roche, Mannheim, Germany). Cells were incubated on ice for 10 min and centrifuged at 14,000×*g* at 4 °C for 10 min. An equal amount of protein was run on polyacrylamide gels, transferred semidry to polyvinylidene difluoride membranes (Amersham, Braunschweig, Germany), and detected using an enhanced chemiluminescense system (Amersham, Braunschweig, Germany). Afterwards, the membranes were stripped and used for ß-actin to ensure equal protein amounts. All used antibodies were purchased from Abcam (Abcam, Cambridge, UK), except anti-ß-actin antibody (Sigma-Aldrich GmbH, Germany), and used according to the manufacturer's instructions.

Analysis of cell surface marker expression by flow cytometry

The antibodies applied included PE-, FITC-, or APC-conjugated CD133/2 (clone 293C3) and IgG2B (provided by Miltenyi Biotech, Bergisch Gladbach, Germany), IgG2a, and CD24 (provided by BD Biosciences, Heidelberg, Germany) and Bcrp1/ABCG2 (R&D Systems, Wiesbaden, Germany). Cells were incubated in PBS containing 0.5 % albumin bovine (BSA) and 0.02 % NaN_3 with fluorescence-conjugated primary antibody; isotype-matched mouse immunoglobulins served as controls. Dead cells were eliminated by using propidium iodide staining at a concentration of 10 μg/ml. Samples were analyzed using a FACS-Calibur flow cytometer and CellQuest software (BD Biosciences, Heidelberg, Germany) or BD-LSRII flow cytometer (in combination with Hoechst staining) (BD Biosciences, Heidelberg, Germany) and FlowJo software (Treestar Inc., Ashland, USA).

Statistical analysis

Statistical evaluation was performed using the paired student's *t* test or ANOVA test (Microcal Origin) with $*p<0.05$ considered to be significant and $**p<0.001$ to be highly significant.

Results

The human pancreatic adenocarcinoma cell line L3.6pl contains a distinct side population of cells

In some tumor entities, cells with CSC characteristics have been isolated based on their ability to efflux the Hoechst 33342 dye. These cells are generally referred to as "side-population" (SP) cells. It has been shown that often times, similar subpopulations can be found in cell lines. The aggressively metastatic pancreatic cell line L3.6pl was examined for the existence of SP cells. Verapamil hydrochloride, which blocks transporters of the ABC family and abrogates the ability to efflux the dye, served as control. The cell line contains a distinct proportion of SP cells (0.9 (±0.22) %) that are sensitive to verapamil hydrochloride (SP content in flow cytometry drops to 0.16 (±0.11) %) (L3.6pl versus L3.6pl+ verapamil, $**p<0.001$) (Fig. 1a, b, c).

To analyze the potential ability of SP cells to give rise to non-SP cells, the SP and the non-SP subpopulations of L3.6pl cells were cultivated for 2 weeks and passaged two times before reanalysis with Hoechst 33342 staining. Analysis by flow cytometry demonstrated that SP cells were able to give rise to both SP (6.53 (±3.92) %) and non-SP cells (93.47 (±3.92) %) (SP versus non-SP, $**p<0.001$) (Fig. 1d). For each reanalysis by FACS, the proportions of SP and non-SP cells were comparable to the initial distribution ratio of both subpopulations. By contrast, isolated non-SP cells of L3.6pl were not able to regenerate SP subpopulations, but were capable of proliferating in vitro (not shown).

Side population cells of L3.6pl induce faster and more aggressive orthotopic tumor growth with higher rates of metastases in vivo

To evaluate the tumor-initiating potential of SP vs. non-SP cells, 1×10^5 SP, non-SP, or unsorted L3.6pl cells were injected into the pancreas of male athymic BALB/c nu/nu mice. Orthotopic tumor growth was estimated by transcutaneous palpation and caliper measurement. At day 34, tumors were measured during necropsy. Between day 31 and 34 after tumor cell injection, only SP cell-derived tumors entered an exponential phase of tumor growth and were found to have significantly outgrown tumors of the other groups (Fig. 2a). Following sacrifice, primary pancreatic tumors derived from the non-SP, unsorted L3.6pl, and SP group showed a mean mass of 0.51 (±0.29)g, 0.98 (±0.28)g, and 1.64 (±0.20)g, respectively (SP versus non-SP, $**p<0.001$; unsorted L3.6pl versus SP, $**p<0.001$; unsorted L3.6pl versus non-SP, $*p=0.01$) (Fig. 2b, c).

The liver and lymph nodes of tumor-implanted mice were also examined for metastatic disease after sacrifice by observation and histology (Table 1). Following orthotopic injection of SP cells into the pancreas, all animals presented with large metastases in the liver and lymph nodes, whereas animals injected with non-SP cells showed only one animal with liver metastases, and 2 out of 10 animals presented with lymph node metastases (SP vs. non-SP group, both liver and lymph node metastases $**p<0.001$). The distribution pattern of metastases following orthotopic injection of unsorted L3.6pl cells

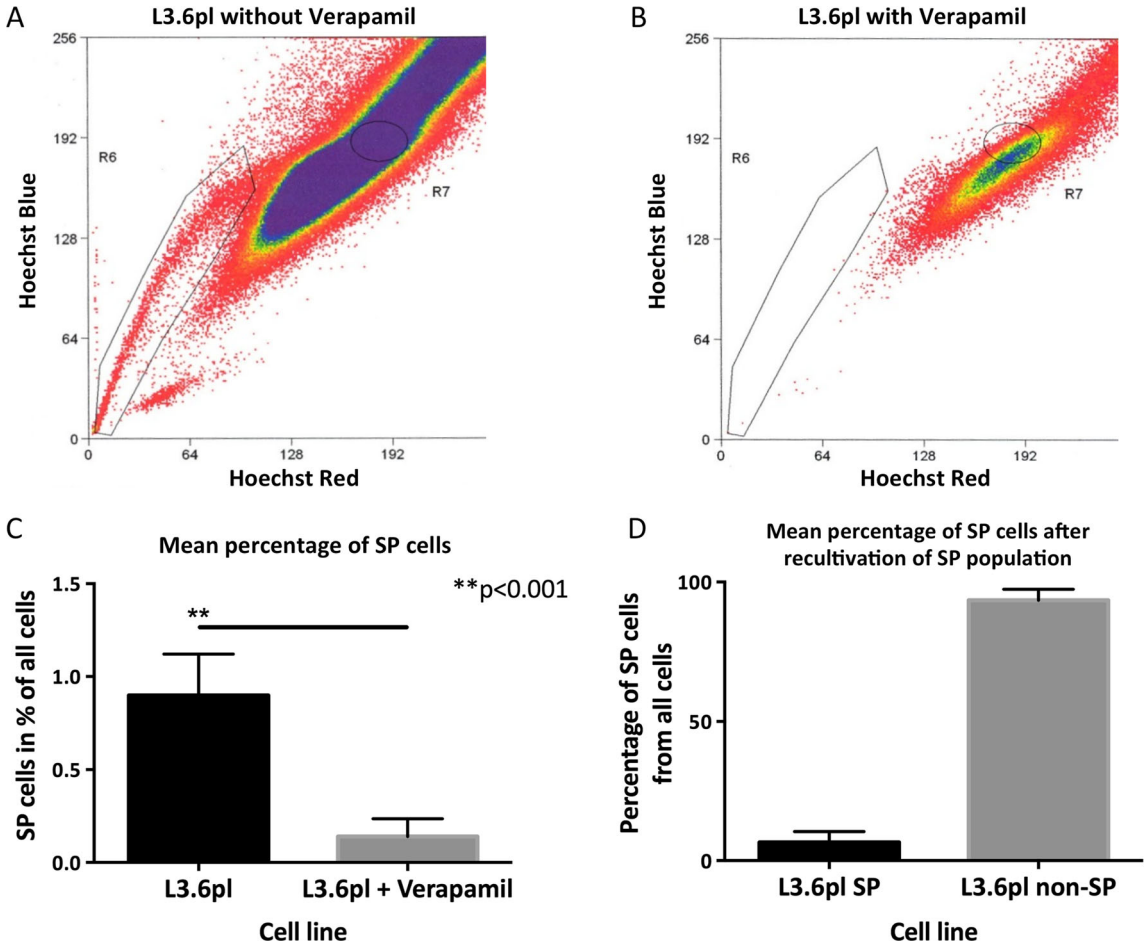

Fig. 1 Identification and isolation of a distinct side population in L3.6pl. **a** SP cells were identified in L3.6pl cells following staining with Hoechst 33342 by flow cytometry analysis using dual-wavelength assessment (*blue* and *red*; SP cells in *gated area*). **b** Adding verapamil to block the ABCG2-mediated efflux of dye served as negative control and successfully diminished the percentage of SP cells in the gated area. **c** In repeated experiments, SP cells were present in cultured L3.6pl with a mean percentage of 0.9 (±0.22)%. Adding of verapamil revealed a reduction of mean SP content to 0.16 (±0.11)% of total cell count (L3.6pl versus L3.6pl+verapamil: $^{**}p<0.001$). **d** After SP cells were isolated by fluorescence-activated cell sorting of L3.6pl SP cells, these cells were cultured for 2 weeks and passaged twice. Thereafter, the cells were reanalyzed for SP content. SP cells were able to produce differentiating non-SP cells and to self-renew (6.53 (±3.92)% SP cells; 93.47 (±3.92)% non-SP cells; $^{**}p<0.001$)

was similar to previously reported results [15]. In our study, 6 out of 13 animals showed liver metastases and 11 out of 13 animals presented with lymph node metastases.

Pancreatic tumors, liver metastases, and the respective surrounding tissue were analyzed by microscopy after H&E staining on paraffin sections (Fig. 2c). Pancreatic tumors derived from unsorted L3.6pl cells commonly showed extensive central necrosis, as a result of aggressive cell proliferation and tissue invasion. Primary pancreatic tumors derived from SP cells resulted in even larger central necrotic areas (64.28 (±13)%), whereas pancreatic tumors following injection of non-SP cells were markedly less necrotic in the center (19.66 (±15.63)%; necrosis SP versus non-SP, $^{**}p<0.001$). H&E staining revealed an infiltrative growth pattern only in liver metastases of SP cell-derived pancreatic carcinoma, leading to hypoxic damage of the ambient liver tissue (not shown). Tumors from non-SP cells of L3.6pl showed better differentiation in H&E stains as compared to unsorted L3.6pl and SP cells. All groups showed significant tumor growth after cell implantation into the pancreas, even the non-SP group. Therefore, while all cell lines showed tumorigenicity in vivo, the SP cells produced faster growing tumors with higher rates of metastases.

Side population cells show a transcriptome consistent with enhanced tumorigenesis

To further characterize differences between the genotypes of SP and non-SP cells, transcriptomic profiling was performed using Affymetrix© HuGene ST 1.0 DNA microarrays. After running quality control steps, the array data was analyzed using two different approaches: classical RMA normalization

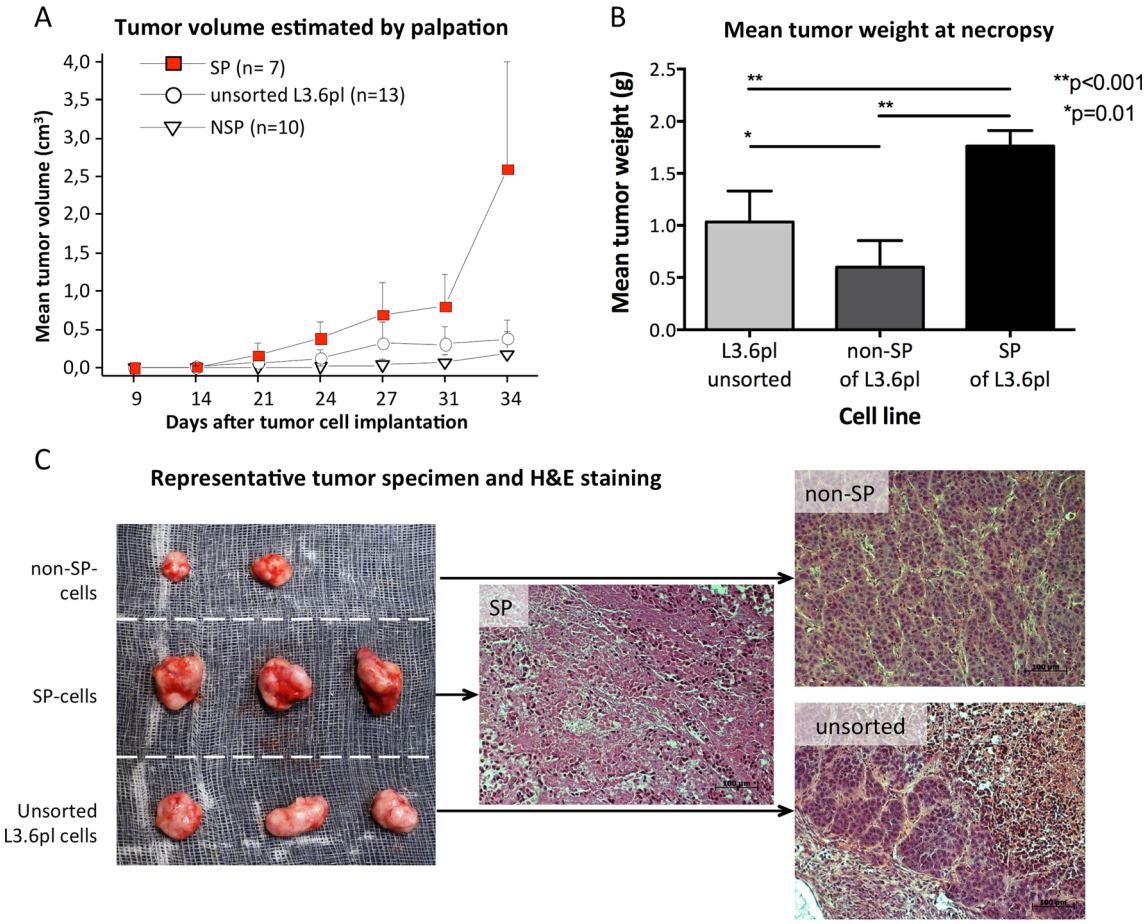

Fig. 2 Tumor formation following orthotopic injection of SP vs. non-SP vs. unsorted L3.6pl. Nu/nu mice were injected orthotopically with 1×10^5 of each cell line, respectively. Tumor size was estimated by transcutaneous palpation and caliper measurement. On day 34, all mice were sacrificed and tumor size measured at necropsy. **a** There was a significant increase in primary tumor growth between day 31 and 34 in the SP group, which led to bigger primary tumors (**b**, **c**) as compared to the non-SP and unsorted L3.6pl group (non-SP-derived tumor 0.51 (±0.29)g; unsorted L3.6pl-derived tumor 0.98 (±0.28)g; SP-derived tumor 1.64 (±0.2)g, SP versus non-SP, $^{**}p<0.001$; unsorted L3.6pl versus SP, $^{**}p<0.001$; unsorted L3.6pl versus non-SP, $^{*}p=0.01$). Results from the metastasization analysis are shown in Table 1. **c** H&E staining of the tumors revealed larger areas of necrosis in SP tumors as compared to non-SP tumors. Tumors derived from SP cells also showed a poorer grade of differentiation in contrast to the highly differentiated tumors that resulted from implantation of non-SP cells

and filtering for significantly differential genes and, in addition, evaluation using the Genomatix Software suite.

Table 1 Distribution of liver and lymph node metastases by experimental group. The table depicts results from the ex vivo analysis of metastasization status in animals following orthotopic tumor cell injection with unsorted L3.6pl, SP of L3.6pl, and non-SP of L3.6pl, respectively (shown are number of positive animals over total number of animals, $^{**}p<0.001$ for both liver and lymph node metastases regarding SP vs. non-SP)

Group	Animals with liver metastasis	Animals with lymph node metastasis
Unsorted L3.6pl	6/13	11/13
SP of L3.6pl	7/7	7/7
Non-SP of L3.6pl	1/10	2/10

RMA analysis yielded transcriptional differences in more than 1,357 genes with a higher proportion of noncoding RNAs than seen in non-SP cells (supplementary data Fig. S1, Table S1). Filtering for a Log_2 1-fold change resulted in a list of 91 genes, with more genes upregulated than downregulated (74 up and 17 down).

SP cells have been shown to positively correlate with tumorigenicity, differentiation, metastasis, and chemotherapy resistance in tumor cells: specifically *AKR1B10*, *ABCG2*, *EID3*, *miRNA221*, *GDF15, and miRNA-21. AKR1B10* RNA in SP cells showed the highest difference in expression level as compared to non-SP cells showing a $\log_2$ fold change of 3.787. The gene encoding for the *ABCG2* drug transporter was upregulated with a $\log_2$ fold change of 2.48, followed by *EID3* ($\log_2$ fold change of 1.771), *microRNA221* ($\log_2$ fold change of 1.742), *GDF15* ($\log_2$ fold change of 1.589), and *micro RNA21* ($\log_2$ fold change of 1.427).

The transcriptomic data was then analyzed further to identify regulatory pathways and gene networks linked to the generation and maintenance of the SP phenotype. Genomatix software (ChipInspector and GePS) was used to identify regulatory pathways that differ significantly between the two cell types. ChipInspector, which in contrast to RMA uses a single probe approach for the identification of significantly dysregulated genes, found 1,087 genes differentially expressed between the two lines (Materials and Methods). These genes were then directly analyzed with additional Genomatix tools. GePS was used to generate and visualize pathways and networks that significantly differ between the SP and non-SP cell populations. The results identified significant alterations in genes associated with the WNT, Notch, and EGF(R) signaling pathways supporting the premise that these cells represent CSCs [1] (Table 2 and Fig. 3).

Table 2 Differentially expressed Wnt, Notch, and EGF pathway genes in SP vs non-SP cells. (*ID* Entrez ID, *Genomatix* Chipinspector normalized data, *RMA* RMA normalized data, normal scale)

	Gene	ID	Genomatix	RMA
Wnt pathway	WNT5	7474	2.57	2.48
	DKK1	22943	1.81	1.46
	DKK3	27122	−1.51	−1.97
	FZD5	7855	−1.56	−1.34
	FZD7	8324	1.86	−1.04
	LRP1	4035	−1.64	−1.56
	JUP	3728	−1.43	−1.15
	MAP1B	4131	2.66	2.70
	PRKCB	5579	−1.55	−1.38
	CDK1	983	1.80	1.36
	EP300	2033	1.60	1.03
	CDC25	995	1.92	1.30
	KREMEN1	83999	−1.51	−1.28
Notch pathway	CNTN1	1272	−1.71	−1.57
	DLL1	28514	−1.65	−1.38
	ADAM17	6868	1.52	1.31
	JAG1	182	1.71	1.33
	JAG2	3714	−1.83	−1.61
	APH1B	83464	−1.68	−1.46
	LFNG	3955	−2.00	−1.50
	NOTCH3	4854	2.16	1.90
	MAML2	84441	−1.58	−1.48
EGF pathway	EGF	1950	1.93	1.86
	EGFR	1956	−1.53	−1.44
	MAP3K2	10746	2.14	1.15
	MAP3K14	9020	1.71	1.30
	PTRRR	5801	1.99	1.89
	CAV-1	857	−1.75	−1.67
	CAV-2	858	−1.53	−1.37

Development of resistance to Gemcitabine and 5-FU leads to alterations in the proportion of side population, $ABCG2^+$, and $CD24^+$ cells but no change in the proportion of $CD133^+$ cells

Resistance to chemotherapy is considered an attribute of CSCs. To evaluate the contribution of SP cells from L3.6pl towards chemoresistance, gemcitabine- and 5-FU-resistant L3.6pl cells were established.

After continuous treatment with gemcitabine, the IC_{50} significantly increased from 6.11 (±0.93)ng/ml in native L3.6pl to 119.77 (±5.12)ng/ml demonstrating increased resistance to gemcitabine thus termed L3.6pl-Gem_{res} (L3.6pl versus L3.6pl-Gem_{res}, $^{**}p<0.001$). With increasing resistance to gemcitabine, the percentage of SP cells rose from 0.9 (±0.22)% in untreated cells to 5.38 (±0.99)% in L3.6pl-Gem_{res} cells (L3.6pl versus L3.6pl-Gem_{res}, $^{**}p<0.001$). Accordingly, the proportion of cells positive for the drug efflux symporter ABCG2 increased significantly after gemcitabine treatment from 0.86 (±0.27)% in L3.6pl cells to 2.83 (±0.8)% in L3.6pl-Gem_{res} cells ($^{**}p<0.001$, Fig. 4b). However, double staining for Hoechst efflux and positivity for ABCG2 using flow cytometry revealed that only 13.95 % of SP cells were positive for ABCG2 (not shown). Therefore, other drug efflux transporters may be responsible for the SP phenotype and further mechanisms of resistance other than drug efflux may be responsible for the gemcitabine resistance seen here.

Intriguingly, no significant difference was observed between L3.6pl and L3.6pl-Gem_{res} cells with regards to their contents of $CD133^+$ cells (Fig. 4b). To add to the impression that SP cells are distinct from the known pancreatic cancer stem cells population isolated by positivity for CD133, Western blotting revealed no correlation between the subpopulations of SP cells and $CD133^+$ cells (Fig. 4c). Here, CD133 even appears to be expressed at a higher level in the non-SP population.

With regards to CD24, another proposed CSC marker in pancreatic cancer, treatment with gemcitabine resulted in an increase of CD24 positive cells from 0.02 (±0.01)% in L3.6pl to 1.06 (±0.09)% in L3.6pl-Gem_{res} cells ($^{**}p<0.001$, Fig. 4b). No change in the contents of CD44 and ESA, two other markers that, in combination with CD24, have been suggested to identify CSCs of pancreatic cancer, were observed (not shown). However, only the simultaneous expression of CD24, CD44, and ESA has been demonstrated to mark potential pancreatic CSC.

After continuous treatment with 5-FU, the IC_{50} significantly increased from 0.1 (±0.01)μg/ml in native L3.6pl to 1.52 (±0.39)μg/ml in L3.6pl-5-FU_{res} ($^{*}p<0.05$). With acquisition of resistance to 5-FU, the SP fraction decreased significantly from 0.9 (±0.22)% to 0.45 (±0.14)% ($^{*}p<0.005$, Fig. 4a) whereas no significant difference was observed in the content of $ABCG2^+$ and $CD133^+$ cells, respectively (Fig. 4b). After

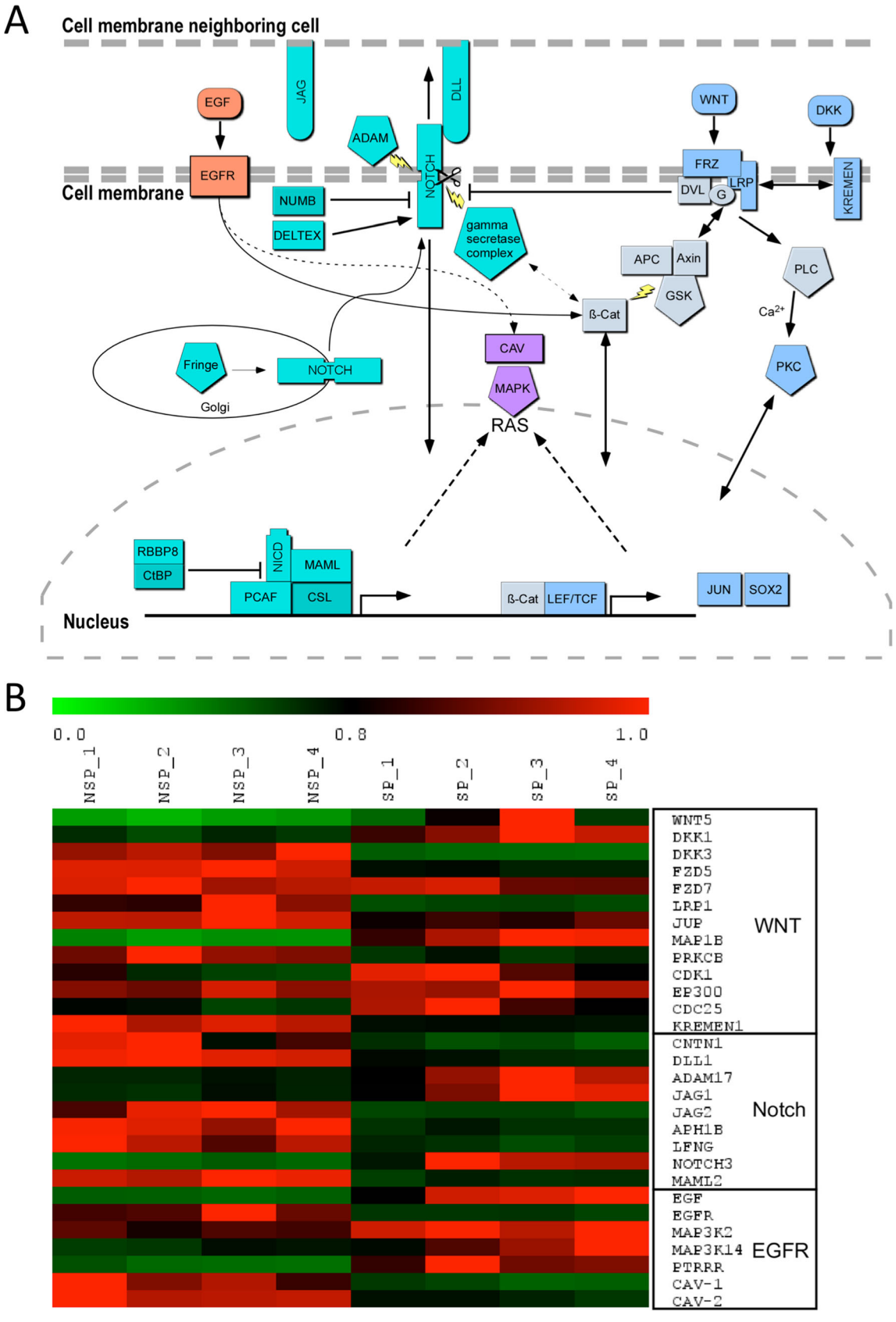
A
Cell membrane neighboring cell
JAG
DLL
EGF
ADAM
NOTCH
WNT
DKK
FRZ
EGFR
DVL
G
LRP
KREMEN
Cell membrane
NUMB
DELTEX
gamma secretase complex
APC
Axin
PLC
GSK
ß-Cat
Ca2+
CAV
Fringe
NOTCH
PKC
MAPK
Golgi
RAS
RBBP8
CtBP
NICD
MAML
PCAF
CSL
ß-Cat
LEF/TCF
JUN
SOX2
Nucleus
B
0.0
0.8
1.0
NSP_1
NSP_2
NSP_3
NSP_4
SP_1
SP_2
SP_3
SP_4
WNT5
DKK1
DKK3
FZD5
FZD7
LRP1
JUP
MAP1B
PRKCB
CDK1
EP300
CDC25
KREMEN1
WNT
CNTN1
DLL1
ADAM17
JAG1
JAG2
APH1B
LFNG
NOTCH3
MAML2
Notch
EGF
EGFR
MAP3K2
MAP3K14
PTRRR
CAV-1
CAV-2
EGFR

◀ **Fig. 3** **a** Overview of differentially expressed pathways: EGF(R) (*red*), NOTCH (*cyan*), WNT (*blue*), and RAS-activated downstream targets (*purple*). Genes shown in *transparency* are not differentially expressed. Enzymes are presented as *pentagonal shapes*, ligands as *rounded rectangles*. In canonical WNT signaling, WNT ligands bind to a Frizzled (*FRZ*) receptor complex, which causes Dishevelled (*DVL*) to bind Axin from the APC/Axin/GS3K ß-catenin destruction complex. This in turn leads to ß-catenin entering the nucleus where it binds the TCF/LEF transcription factors, leading to gene expression and downstream activation of mitogen activated kinases (*MAPK*) via RAS signaling. DKK, of which DKK1 is also upregulated in SP cells, can inhibit WNT by removing LRP from the Frizzled complex through KREMEN. In noncanonical Ca^{2+} WNT signaling, the WNT-FRZ complex activates phospholipase C (*PLC*) via a bound G-protein (*G*). This leads to changes in Ca^{2+} levels, activating proteinkinase c (*PKC*). The NOTCH receptor is activated on contact with a neighboring cell's jagged (*JAG*) or delta like (*DLL*) receptors/ligands. NOTCH is cleaved by A Disintegrin and Metalloprotease (*ADAMs*) in cooperation with the intracellular gamma secretase complex. Upon cleavage, the NOTCH intracellular domain (*NICD*) is transported to the nucleus where it acts as a transcriptional activator together with MAML, PCAF, CSL, and is inhibited by CtBP. The extracellular domain is taken up by the neighboring cell. Notch signaling is regulated by NUMB and Deltex. Regeneration of NOTCH in the golgi apparatus is carried out by FRINGE proteins such as lunatic fringe (*LFNG*). Epithelial growth factor (*EGF*) binds to the EGF Receptor (*EGFR*), which has widespread effects on the cell. EGFR can also activate β-catenin [54]. Shown here is the downstream activation of RAS via Integrin/Caveolin (*CAV*) signaling which leads to changes in MAPK activation. **b** Heatmap of relative gene expressions for the pathway genes (see also Table 2). Scanned signal strengths are expressed as relative values for each gene with the strongest signal being set to 1. (*SP* side population arrays 1-4, *NSP* nonside population arrays 1-4)

treatment with 5-FU, the proportion of $CD24^+$ cells was highly elevated in this resistant variant: L3.6pl cells showed 0.02 (±0.01)% of $CD24^+$ cells as compared to 6.71 (±0.16)% in L3.6pl-5-FU_{res} (**$p<0.001$). Again, no changes in the contents of CD44 and ESA were observed.

AKR1B10 is increased at the protein level in L3.6pl side population cells and L3.6pl cells with increased resistance to gemcitabine

AKR1B10 expression has been described to be associated with increased tumorigenesis as well as drug resistance in several cancer entities [22]. In the Affymetrix analysis, the *AKR1B10* gene showed the highest upregulation of all genes in the SP of L3.6pl. Thus, we decided to further examine *AKR1B10* expression on protein level by Western blotting in unsorted L3.6pl and its chemoresistant variants as well as the side populations isolated from unsorted L3.6pl and L3.6pl-Gem_{res} as well as the non-SP cells of L3.6pl. It became evident that *AKR1B10* is expressed in unsorted L3.6pl and is highly upregulated in gemcitabine-resistant L3.6pl-Gem_{res} but is not expressed in the 5-FU-resistant L3.6pl-5-FU_{res} (Fig. 5a). The expression of *AKR1B10* in L3.6pl is mainly due to the highly upregulated expression of this protein in the SP fraction of L3.6pl with only slight expression seen in the non-SP fraction of cells (Fig. 5b). This confirms the result from the gene array analysis of differential AKR1B10 expression on protein level. The effect of elevated AKR1B10 is further augmented in the gemcitabine-resistant cell line L3.6pl-Gem_{res} in which the expression of *AKR1B10* is almost exclusive to the side population of this resistant variant.

Discussion

The hypothesis of a subpopulation of tumor cells with inherent stem cell characteristics has been used to help explain phenomenon observed in cancer biology, such as the initiation of tumor growth, tissue invasion, formation of metastases, and chemo and radioresistance [23]. In the search for these "cancer stem cells (CSC)", multiple approaches have been applied in hematologic and solid malignancies. Using surface marker combinations used to identify nonmalignant stem cells, such as $CD34^+/CD38^-$, $CD44^{high}/CD24^{low}/Lin^-$ or $CD133^+$, tumor cells with stem cell-like characteristics have been isolated [7, 24–27]. A different approach makes use of the increased ability of stem cells to efflux fluorescent dye [28]. The so-called "side population" (SP) of cells obtained by this method can show stem cell characteristics. Recent reports have suggested that these SP cells may represent CSCs in diverse malignancies [29] including hepatocellular carcinoma [30], melanoma [31], glioma [32], esophageal cancer [33], and lung carcinoma [34]. In the present study, we detected and characterized a unique SP present in the highly metastatic pancreatic adenocarcinoma cell line L3.6pl by their ability to efflux Hoechst 33342 dye. The proportion of the side subpopulation was 0.9 (±0.22)% of unsorted L3.6pl cells (Fig. 1a), which lies in the proportional range of cancer stem cells identified in other solid tumor entities [35]. L3.6pl SP cells were able to self-renew and to differentiate into non-SP cells after 2 weeks of cultivation and two passages—established criteria for potential CSCs (Fig. 1b).

Side populations have been described in other pancreatic cancer cell lines previously, such as PANC-1, Capan-2, KP-1NL, and MIAPaCa2. They have been examined with respect to epithelial to mesenchymal transition (EMT), invasion, formation of metastasis, and gemcitabine resistance [36, 37]. However, the tumor growth characteristics of these pancreatic cancer SP cells in vivo have not been assessed thoroughly and no information about genetic alterations differing these cells from the non-SP cells have been published. However, this information is deemed indispensable in order to find a specific treatment targeting these tumor cells with stem cell characteristics.

It has been previously shown that only a few SP cells are capable of inducing tumor formation, whereas a large amount of non-SP cells are generally needed to achieve the same

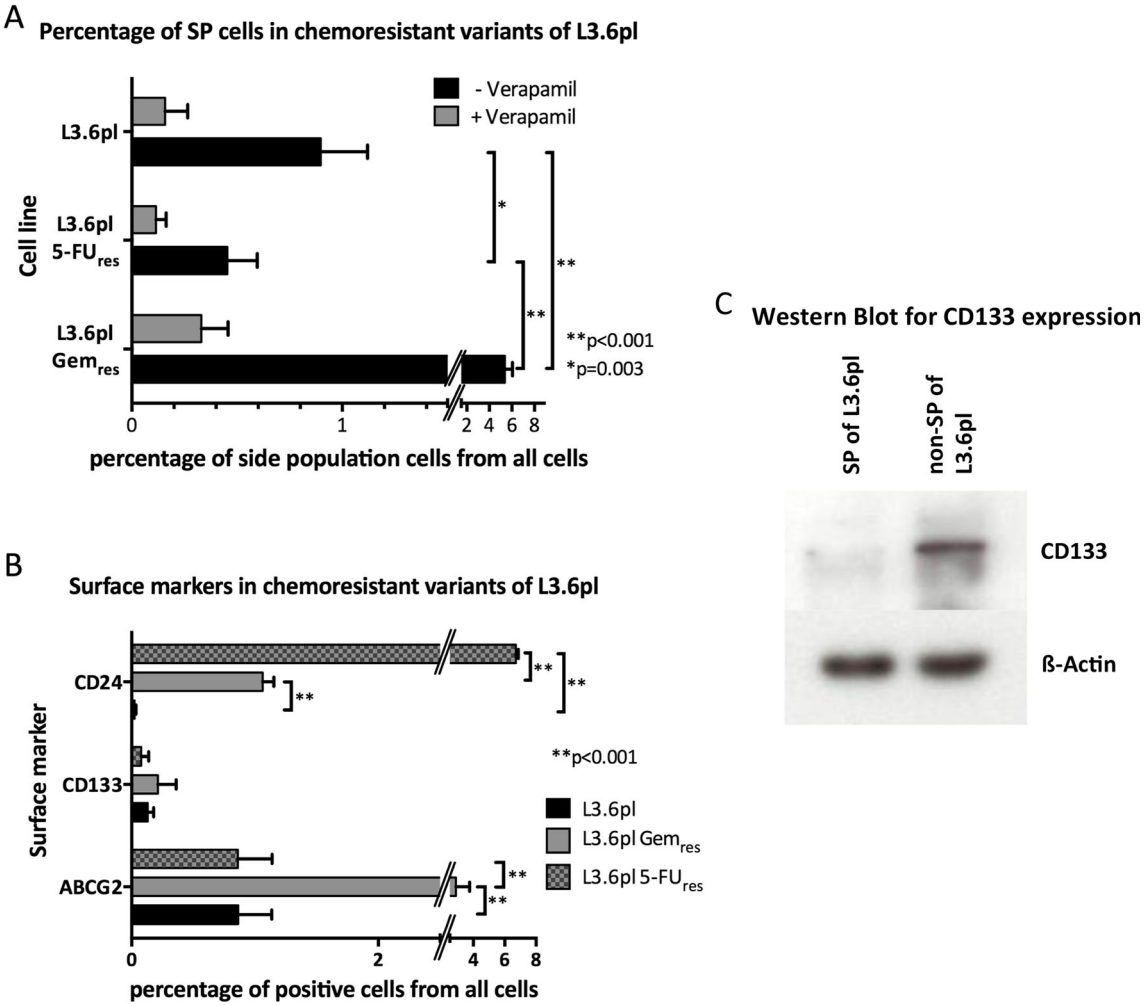

Fig. 4 Effect of chemotherapy on SP and expression of surface markers associated with stemness. **a** Depicts a flow cytometry analysis for SP content of unsorted L3.6pl, L3.6pl-Gem$_{res}$, and L3.6pl-5-FU$_{res}$. After continuous treatment of L3.6pl cells with gemcitabine, the SP fraction strikingly increased from 0.9 (±0.22)% to 5.38 (±0.84)% (L3.6pl versus L3.6pl-Gem$_{res}$, both without verapamil, $^{**}p<0.001$). With acquisition of increased resistance to 5-FU, the SP fraction decreased significantly by about 50 % from 0.9 (±0.22)% to 0.45 (±0.14)% (L3.6pl versus L3.6pl-5-FU$_{res}$, both without verapamil, $^{**}p<0.001$). **b** shows a flow cytometry analysis for the surface markers CD24, CD133, and ABCG2 on native and chemotherapeutically pretreated variants of L3.6pl. The content of ABCG2 positive cells in L3.6pl was significantly increased following gemcitabine treatment (0.86 (±0.27)% in native L3.6pl to 2.83 (±0.8)% in L3.6pl-Gem$_{res}$, $^{**}p<0.001$) whereas it remained unaltered following 5-FU treatment. Similarly, CD24 content rose from 0.02 (±0.01)% in L3.6pl to 1.06 (±0.09)% in L3.6pl-Gem$_{res}$, ($^{**}p<0.001$). This effect was even more profound under 5-FU treatment of L3.6pl, where the proportion of CD24 positive cells rose to 6.71 (±0.16)% ($^{**}p<0.001$). No significant difference was observed in regard to the proportion of CD133^{+} cells independent of the chemotherapy used. This unexpected result was followed by a Western blot analysis to check for the baseline expression of CD133 in nonpretreated SP and non-SP cells of L3.6pl depicted in **c**. Western blot demonstrates only minimal to no expression of CD133 in SP and mild expression in non-SP cells of L3.6pl

tumor growth in xenografts [30, 34]. In our experiments, orthotopic injection of SP cells of L3.6pl resulted in significantly larger tumors and higher incidence of liver and lymph node metastases as compared to unsorted L3.6pl and non-SP of L3.6pl. This provides further evidence for the CSC characteristics of the SP fraction. More aggressive growth characteristics were indicated by the observation of significantly larger areas of central necrosis in SP cell-derived tumors as well as a lower grade of differentiation (Fig. 2; Table 1).

The increased drug efflux of SP cells is directly connected to their resistance to chemotherapy. The drug symporter ABCG2 is considered the main determinant of side population cells after Hoechst 33342 staining as demonstrated in hematopoietic stem cells [38]. Cancer cells overexpressing ABCG2 are more resistant to mitoxantrone, daunorubicin, doxorubicin, topotecan in breast cancer, and 5-fluorouracil (5-FU) and gemcitabine in liver cancer, respectively [35, 39]. However, in L3.6pl cells, the SP phenotype appears to be determined only in part by ABCG2 expression, as only about 14 % of SP cells showed expression of ABCG2. Other drug efflux symporters from the ABC superfamily may contribute to the SPs seen here. Of these, ABCB6 and ABCC2 were found to be upregulated in the microarray analysis, although not significantly, in SP versus non-SP cells of L3.6pl. Others have also

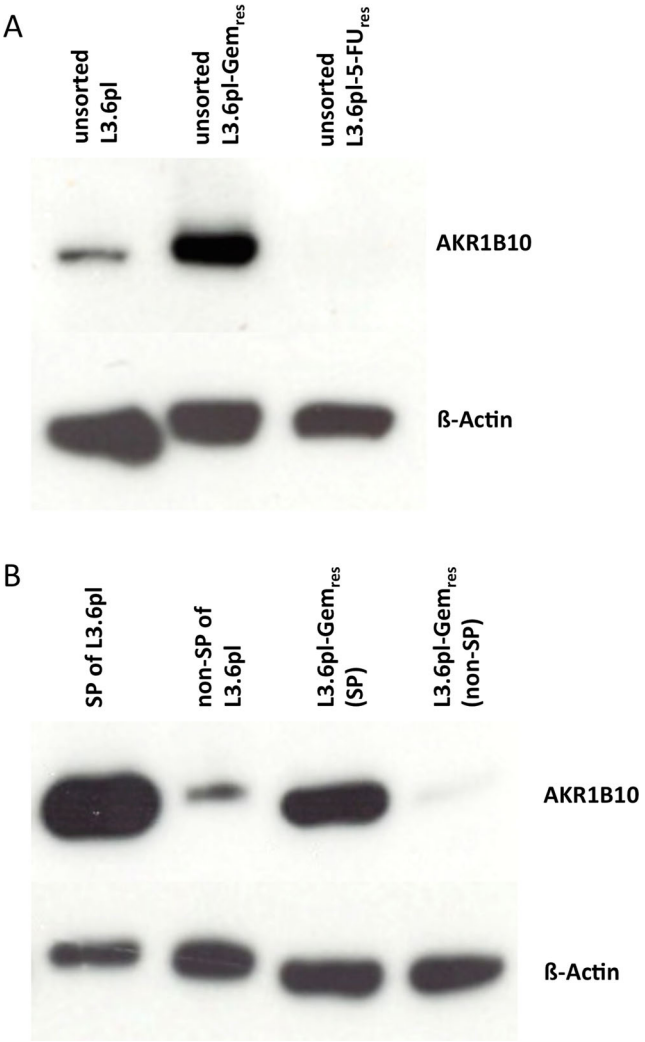

Fig. 5 Western blot analysis for changes in AKR1B10 expression following chemotherapeutic treatment of L3.6pl. **a** Shows a Western blot analysis for expression of AKR1B10, a gene associated with detoxification of chemotherapeutic agents, in unsorted L3.6pl, unsorted L3.6pl-Gem$_{res}$, and unsorted L3.6pl-5-FU$_{res}$. The analysis demonstrates elevated expression of AKR1B10 in L3.6pl following gemcitabine but not 5-FU treatment. As seen in **b**, this effect can be attributed to higher expression of AKR1B10 in side population cells of L3.6pl, which are enriched under gemcitabine treatment (as seen in Fig. 4b). This confirms the results from the gene array analysis, where AKR1B10 was the gene with the highest upregulation in SP vs. non-SP cells. The effect of elevated AKR1B10 expression in SP cells appears to be even more profound after gemcitabine treatment as seen by the minimal band for AKR1B10 in non-SP cells of L3.6pl-Gem$_{res}$. Hence, AKR1B10 expression became almost exclusive to the side population of L3.6pl under treatment with gemcitabine

demonstrated the lack of exclusivity of ABCG2 to efflux Hoechst 33342 dye. Human umbilical cord blood-derived SP cells were ABCG2 negative after isolation by the Hoechst 33342 protocol [40].

To investigate the role of SP cells in L3.6pl with respect to therapy resistance, we generated L3.6pl-Gem$_{res}$, a gemcitabine-resistant cell line and L3.6pl-5-FU$_{res}$, a 5-FU-resistant cell line and isolated side populations from both resistant cell lines. The content of SP cells was found to be significantly elevated in L3.6pl-Gem$_{res}$ as compared to their drug sensitive counterparts (Fig. 4a). In both L3.6pl and L3.6pl-Gem$_{res}$ cells, ABCG2 was enriched in the respective SPs as compared to the non-SPs. After continuous treatment with 5-FU, the percentage of SP cells was decreased. This suggests that 5-FU treatment might effectively diminish the SP content of this cancer cell line and that the SP fraction of cells correlates only with gemcitabine resistance.

Recently, superiority of 5-FU- over gemcitabine-based chemotherapeutic treatment concerning overall- and progression-free survival in patients with metastatic pancreatic cancer was proven [41]. In our animal studies, application of large numbers of SP cells resulted in the highest rates of metastasis. Metastatic disease in patients suffering from pancreatic cancer might therefore represent a tumor state associated with proportionally large amounts of SP cells. Furthermore, SP cells showed sensitivity only to 5-FU but not to gemcitabine treatment in vitro. A link between the effective abrogation of SP cells by 5-FU treatment observed here and the clinical superiority of 5-FU in patients with metastatic disease seems likely and should be subjected to further studies.

CD133 is the most commonly applied marker for solid tumor stem cells [11]; however, its use in this regard remains controversial. Shmelkov et al. showed that CD133 expression is not restricted to stem cells in metastatic colon cancer [42], and the general use of CD133 as a CSC marker for colorectal carcinoma has been criticized [43]. We show here that L3.6pl SP cells are negative for CD133 (Fig. 4c), but still demonstrate characteristics of CSCs. We observed no difference with respect to the percentage of $CD133^+$ cells before or after treatment with gemcitabine or 5-FU. These results stand in contrast to previous studies in which gemcitabine treatment enriched for CD133+ cells [13].

These disparate results may be explained in part by the methodologies used for selecting the cells. The different approaches may define different subpopulations of CSC-like tumor cells within the same tumor cell line.

To further characterize potential stem cell traits and the development of drug resistance in SP cells, gene array studies were used to reveal differences in the expression profile of specific cancer-associated genes and regulatory pathways significantly altered between SP cells and non-SP cells.

The CSC hypothesis suggests that reactivation of developmental signaling cascades, combined with increased DNA repair mechanisms, and ABC transporter-mediated drug efflux may underlie the biology seen in CSCs. Comparison of the transcriptome of SP vs non-SP cells followed by pathway mapping identified a significant change in the NOTCH, Wnt, and EGFR signaling pathways. These pathways regulate development and tissue maintenance in the adult, and control

cell fate by regulating proliferation, cell death, polarity, senescence, and adhesion, as well as the expression of cell type-specific proteins and transcription factors (Fig. 3).

Aldo-keto reductase family 1 B10 (*AKR1B10*) showed the highest increase in expression level in SP cells in the Affymetrix analysis, confirmed by Western blotting (supplements Table S1, Fig. 5b). Two other members of the AKR superfamily, AKR1C2 and AKR1C3 were also increased in SP (2-fold change of 0.97 and 1.1). The aldo-keto reductase superfamily plays a major role in the detoxification of pharmaceuticals, drugs, and xenobiotics [44]. AKR1B10 converts all-trans-retinals to all-trans-retinols, which inhibits retinoic acid-triggered differentiation and increases the ability of cells to proliferate. This mechanism may contribute to the dedifferentiation of tumor cells towards a CSC-like tumor cell [45]. The importance of *AKR1B10* expression for tumor growth has been described in several tumor entities. It is established as a marker of recurrence after surgical treatment in cervical cancer and has been proposed as a marker for non-small cell lung carcinoma in smokers [46]. Silencing of *AKR1B10* effectively inhibits growth of colorectal cancer cells [47]. The biological function of AKR1B10 upregulation in SP cells of L3.6pl especially its potential role in chemoresistance and high proliferative potential of these cells needs to be addressed in further studies.

Additional upregulated genes in L3.6pl SP cells found in the Affymetrix analysis include EP300 interacting inhibitor of differentiation 3 (*EID3*), growth differentiation factor 15 (*GDF15*), *microRNA221*, and *microRNA21* (Table S1). *EID3* acts as an inhibitor of differentiation and thus may contribute to the "stemness" characteristics of SP cells [48]. GDF15 is a member of the TGF-ß superfamily and shows protumorigenic characteristics in several cancer entities including pancreatic [49]. MicroRNAs are believed to contribute to stem cell characteristics through posttranscriptional gene silencing [50] MiRNA21 is discussed to regulate oncogenic processes by targeting tumor suppressor genes responsible for invasion and metastasis [51]. MiRNA221 plays an important role regarding tamoxifen resistance in breast cancer [52]. Antisense inhibition of miRNA221 or miRNA21 leads to increased cell apoptosis and an elevated expression of associated tumor suppressor genes resulting in sensitization of pancreatic adenocarcinoma to gemcitabine [53].

Conclusion

Side-population cells of the human pancreatic cancer cell line L3.6pl represent cells that show high proliferative potential, differentiation, induction of aggressive tumor growth, high rates of metastasis, and are resistant towards gemcitabine. These results suggest that they represent a cell subpopulation with many of the defining characteristics of cancer stem cells. Genes differentially expressed between SP and non-SP cells include several genes linked to more aggressive tumor growth as well as sets of genes linked to the NOTCH, Wnt, and EGFR signaling pathways. The SP of L3.6pl represents a subset of cells that cannot be defined using previously established surface markers for pancreatic CSC, such as CD133. The results suggest that the cells may represent a viable model system for the study of CSCs.

Conflict of interest The authors declare that they have no conflict of interest.

References

1. Pardal R, Clarke MF, Morrison SJ (2003) Applying the principles of stem-cell biology to cancer. Nat Rev Cancer 3:895–902
2. Nowell PC (1976) The clonal evolution of tumor cell populations. Science 194:23–8
3. Reya T, Morrison SJ, Clarke MF, Weissman IL (2001) Stem cells, cancer, and cancer stem cells. Nature 414:105–11
4. Donnenberg VS, Donnenberg AD (2005) Multiple drug resistance in cancer revisited: the cancer stem cell hypothesis. J Clin Pharmacol 45:872–7
5. Bao S, Wu Q, McLendon RE, Hao Y, Shi Q, Hjelmeland AB et al (2006) Glioma stem cells promote radioresistance by preferential activation of the DNA damage response. Nature 444:756–60
6. McDonald SA, Graham TA, Schier S, Wright NA, Alison MR (2009) Stem cells and solid cancers. Virchows Arch 455:1–13
7. Bonnet D, Dick JE (1997) Human acute myeloid leukemia is organized as a hierarchy that originates from a primitive hematopoietic cell. Nat Med 3:730–7
8. Dick JE (2005) Acute myeloid leukemia stem cells. Ann N Y Acad Sci 1044:1–5
9. Bhagwandin VJ, Shay JW (2009) Pancreatic cancer stem cells: fact or fiction? Biochim Biophys Acta 1792:248–59
10. Sergeant G, Vankelecom H, Gremeaux L, Topal B (2009) Role of cancer stem cells in pancreatic ductal adenocarcinoma. Nat Rev Clin Oncol 6:580–6
11. Hermann PC, Bhaskar S, Cioffi M, Heeschen C (2010) Cancer stem cells in solid tumors. Semin Cancer Biol 20:77–84
12. Li C, Heidt DG, Dalerba P, Burant CF, Zhang L, Adsay V et al (2007) Identification of pancreatic cancer stem cells. Cancer Res 67:1030–7
13. Hermann PC, Huber SL, Herrler T, Aicher A, Ellwart JW, Guba M et al (2007) Distinct populations of cancer stem cells determine tumor growth and metastatic activity in human pancreatic cancer. Cell Stem Cell 1:313–23
14. Goodell MA, Brose K, Paradis G, Conner AS, Mulligan RC (1996) Isolation and functional properties of murine hematopoietic stem cells that are replicating in vivo. J Exp Med 183:1797–806
15. Bruns CJ, Harbison MT, Kuniyasu H, Eue I, Fidler IJ (1999) In vivo selection and characterization of metastatic variants from human pancreatic adenocarcinoma by using orthotopic implantation in nude mice. Neoplasia 1:50–62
16. Krebs S, Fischaleck M, Blum H (2009) A simple and loss-free method to remove TRIzol contaminations from minute RNA samples. Anal Biochem 387:136–8
17. Gentleman RC, Carey VJ, Bates DM, Bolstad B, Dettling M, Dudoit S et al (2004) Bioconductor: open software development for computational biology and bioinformatics. Genome Biol 5:R80

18. Irizarry RA, Bolstad BM, Collin F, Cope LM, Hobbs B, Speed TP (2003) Summaries of Affymetrix GeneChip probe level data. Nucleic Acids Res 31:e15
19. Smyth GK (2004) Linear models and empirical bayes methods for assessing differential expression in microarray experiments. Stat Appl Genet Mol Biol;3:Article3
20. Moll AG, Lindenmeyer MT, Kretzler M, Nelson PJ, Zimmer R, Cohen CD (2009) Transcript-specific expression profiles derived from sequence-based analysis of standard microarrays. PLoS ONE 4:e4702
21. Notohamiprodjo S, Djafarzadeh R, Rieth N, Hofstetter M, Jaeckel C, Nelson PJ (2012) Cell surface engineering of renal cell carcinoma with glycosylphosphatidylinositol-anchored TIMP-1 blocks TGF-beta 1 activation and reduces regulatory ID gene expression. Biol Chem 393:1463–70
22. Ebert B, Kisiela M, Wsol V, Maser E (2011) Proteasome inhibitors MG-132 and bortezomib induce AKR1C1, AKR1C3, AKR1B1, and AKR1B10 in human colon cancer cell lines SW-480 and HT-29. Chem Biol Interact 191:239–49
23. Huntly BJ, Gilliland DG (2005) Cancer biology: summing up cancer stem cells. Nature 435:1169–70
24. Lapidot T, Sirard C, Vormoor J, Murdoch B, Hoang T, Caceres-Cortes J et al (1994) A cell initiating human acute myeloid leukaemia after transplantation into SCID mice. Nature 367:645–8
25. Ricci-Vitiani L, Lombardi DG, Pilozzi E, Biffoni M, Todaro M, Peschle C et al (2007) Identification and expansion of human colon-cancer-initiating cells. Nature 445:111–5
26. Singh SK, Hawkins C, Clarke ID, Squire JA, Bayani J, Hide T et al (2004) Identification of human brain tumour initiating cells. Nature 432:396–401
27. Al-Hajj M, Wicha MS, Benito-Hernandez A, Morrison SJ, Clarke MF (2003) Prospective identification of tumorigenic breast cancer cells. Proc Natl Acad Sci U S A 100:3983–8
28. Challen GA, Little MH (2006) A side order of stem cells: the SP phenotype. Stem Cells 24:3–12
29. Wulf GG, Wang RY, Kuehnle I, Weidner D, Marini F, Brenner MK et al (2001) A leukemic stem cell with intrinsic drug efflux capacity in acute myeloid leukemia. Blood 98:1166–73
30. Chiba T, Kita K, Zheng YW, Yokosuka O, Saisho H, Iwama A et al (2006) Side population purified from hepatocellular carcinoma cells harbors cancer stem cell-like properties. Hepatology 44:240–51
31. Dou J, Wen P, Hu W, Li Y, Wu Y, Liu C et al (2009) Identifying tumor stem-like cells in mouse melanoma cell lines by analyzing the characteristics of side population cells. Cell Biol Int 33:807–15
32. Harris MA, Yang H, Low BE, Mukherjee J, Guha A, Bronson RT et al (2008) Cancer stem cells are enriched in the side population cells in a mouse model of glioma. Cancer Res 68:10051–9
33. Zhao Y, Bao Q, Schwarz B, Zhao L, Mysliwietz J, Ellwart J, et al (2014) Stem cell like side populations in esophageal cancer: a source of chemotherapy resistance and metastases. Stem Cells Dev 23:180–92
34. Ho MM, Ng AV, Lam S, Hung JY (2007) Side population in human lung cancer cell lines and tumors is enriched with stem-like cancer cells. Cancer Res 67:4827–33
35. Haraguchi N, Utsunomiya T, Inoue H, Tanaka F, Mimori K, Barnard GF et al (2006) Characterization of a side population of cancer cells from human gastrointestinal system. Stem Cells 24:506–13
36. Kabashima A, Higuchi H, Takaishi H, Matsuzaki Y, Suzuki S, Izumiya M et al (2009) Side population of pancreatic cancer cells predominates in TGF-beta-mediated epithelial to mesenchymal transition and invasion. Int J Cancer 124:2771–9
37. Zhou J, Wang CY, Liu T, Wu B, Zhou F, Xiong JX et al (2008) Persistence of side population cells with high drug efflux capacity in pancreatic cancer. World J Gastroenterol 14:925–30
38. Zhou S, Schuetz JD, Bunting KD, Colapietro AM, Sampath J, Morris JJ et al (2001) The ABC transporter Bcrp1/ABCG2 is expressed in a wide variety of stem cells and is a molecular determinant of the side-population phenotype. Nat Med 7:1028–34
39. Doyle LA, Ross DD (2003) Multidrug resistance mediated by the breast cancer resistance protein BCRP (ABCG2). Oncogene 22:7340–58
40. Alt R, Wilhelm F, Pelz-Ackermann O, Egger D, Niederwieser D, Cross M (2009) ABCG2 expression is correlated neither to side population nor to hematopoietic progenitor function in human umbilical cord blood. Exp Hematol 37:294–301
41. Conroy T, Desseigne F, Ychou M, Bouche O, Guimbaud R, Becouarn Y et al (2011) FOLFIRINOX versus gemcitabine for metastatic pancreatic cancer. N Engl J Med 364:1817–25
42. Shmelkov SV, Butler JM, Hooper AT, Hormigo A, Kushner J, Milde T et al (2008) CD133 expression is not restricted to stem cells, and both CD133+ and CD133− metastatic colon cancer cells initiate tumors. J Clin Invest 118:2111–20
43. Dittfeld C, Dietrich A, Peickert S, Hering S, Baumann M, Grade M et al (2010) CD133 expression is not selective for tumor-initiating or radioresistant cell populations in the CRC cell line HCT-116. Radiother Oncol 94:375–83
44. Barski OA, Tipparaju SM, Bhatnagar A (2008) The aldo-keto reductase superfamily and its role in drug metabolism and detoxification. Drug Metab Rev 40:553–624
45. Diez-Dacal B, Gayarre J, Gharbi S, Timms JF, Coderch C, Gago F, et al (2011) Identification of Aldo-keto reductase AKR1B10 as a selective target for modification and inhibition by prostaglandin A1: implications for anti-tumoral activity. Cancer Res 71:4161–71
46. Fukumoto S, Yamauchi N, Moriguchi H, Hippo Y, Watanabe A, Shibahara J et al (2005) Overexpression of the aldo-keto reductase family protein AKR1B10 is highly correlated with smokers' non-small cell lung carcinomas. Clin Cancer Res 11:1776–85
47. Yan R, Zu X, Ma J, Liu Z, Adeyanju M, Cao D (2007) Aldo-keto reductase family 1 B10 gene silencing results in growth inhibition of colorectal cancer cells: implication for cancer intervention. Int J Cancer 121:2301–6
48. Sasajima Y, Tanaka H, Miyake S, Yuasa Y (2005) A novel EID family member, EID-3, inhibits differentiation and forms a homodimer or heterodimer with EID-2. Biochem Biophys Res Commun 333:969–75
49. Koopmann J, Buckhaults P, Brown DA, Zahurak ML, Sato N, Fukushima N et al (2004) Serum macrophage inhibitory cytokine 1 as a marker of pancreatic and other periampullary cancers. Clin Cancer Res 10:2386–92
50. Zimmerman AL, Wu S (2011) MicroRNAs, cancer and cancer stem cells. Cancer Lett 300:10–9
51. Zhu S, Wu H, Wu F, Nie D, Sheng S, Mo YY (2008) MicroRNA-21 targets tumor suppressor genes in invasion and metastasis. Cell Res 18:350–9
52. Miller TE, Ghoshal K, Ramaswamy B, Roy S, Datta J, Shapiro CL et al (2008) MicroRNA-221/222 confers tamoxifen resistance in breast cancer by targeting p27Kip1. J Biol Chem 283:29897–903
53. Park JK, Lee EJ, Esau C, Schmittgen TD (2009) Antisense inhibition of microRNA-21 or -221 arrests cell cycle, induces apoptosis, and sensitizes the effects of gemcitabine in pancreatic adenocarcinoma. Pancreas 38:e190–9
54. Hu T, Li C (2010) Convergence between Wnt-beta-catenin and EGFR signaling in cancer. Mol Cancer 9:236